Chapter
5.2

Thermal Transport and Temperature Distribution via the Circulation:
A Mathematical Model

Abstract

The conventional core and shell descriptions of temperature distribution in human thermoregulation are not of adequate utility for conditions of metabolic or environmental thermal stress, since "core" temperatures may be 5°C different at different sites in the same person at the same time, and may provide conflicting indications to clinicians.

A new and surprisingly simple model is developed and shown to correctly predict observed dynamics of temperature distribution in surgery and sports medicine examples where the conventional model fails. The governing equations, solved using electrical analog techniques, are based on a novel method of modeling heat transport via the circulation.

Introduction

With thousands of years of recognition of the role of temperature in diagnosis and treatment of disease, it is somewhat surprising that so little is known of the dynamics of thermal transport and temperature distribution, and their effects on thermoregulation. As a result, medical caregivers have incomplete information, which hinders use of more effective therapies, or in some cases, indicates therapies which can be dangerous to the patient. Several of these areas are:

- Treatment of fever by relying on rectal temperature, which may lag arterial temperature by many hours (Chapter 1.7).
- Palpation for fever by relying on skin temperature, which responds in a contra direction to arterial temperature during early stage fever (Chapter 1.9).
- Treatment of an athlete for hyperthermia when the athlete is actually hypothermic, and is in great danger of overcooling.[2] (Chapter 5.3).
- Failure to unmask infectious diseases early enough to prevent unnecessary morbidity and mortality (Chapter 1.1).

Historically, temperature and heat distribution has been viewed from the intuitive and simple to remember concepts of "core" and "shell", where core temperature is interpreted as the tissue temperature several centimeters below skin surface, and the remainder is the cooler shell; with some relative volume variation of each due to environment, exercise, etc.[4] This model adequately represents temperature distribution under quiescent conditions, and normal hemodynamics, since the typical variations of less than a degree from site to site have little clinical significance.

The conventional model fails when there are significant contributions from metabolic activity, environmental influences, failure of thermoregulation, or hemodynamic redistribution. Some of the effects of these perturbations have only recently been capable of observation, due to the recent availability of accurate non-invasive methods of infrared tympanic thermometry[5] and arterial temperature via heat balance at the ear,[6] providing new data on the dynamics of temperature distribution under a variety of conditions previously not possible.

Accordingly, the mathematical model addresses the limitations of the conventional core and shell description by accounting for the creation, transport, and rejection of heat energy and from first principles producing a still very simple model that correctly predicts the dynamic features of thermal transport and temperature distribution.

The key conceptual requirement of the mathematical model is to view the cardiovascular system as the principle transport mechanism for heat energy, in precisely the same fashion as it is used in the transport of oxygen, nutrients, waste products, etc. Heat transport via the circulation is shown to be more than 100 times as effective as heat transfer via diffusion (conduction) in moving energy any appreciable distance. Since metabolizing tissue can generate far more

heat than it can diffuse to the skin, the transport function must be employed to carry the heat energy to all available skin area, when necessary.

An electrical analog method of representation of the governing differential equations was chosen for ease and convenience of model construction, since the topology of the tissues and cardiovascular system is retained. Each major tissue type participating in heat production, transport, or rejection is characterized by its thermal activity properties, and "lumped" into an electrical analog with the identical form of defining equations. High predictive power for the dynamic events studied were obtained with only the following elements:

- Skin of the head
- Mass of the head
- Mass of the internal tissue
- Mass of the muscles
- Skin of the body
- Connecting vasculature

No assumptions were made or elements included for a feedback control model of thermoregulation. The data chosen for model validation and predictive power were all under conditions in which thermoregulation was rendered inactive or "at its stops", i.e. under general anesthesia in the case of a surgical patient, or calling for maximum cooling in the case of a hyperthermic athlete.

METHODS

Thermal diffusion as a transport mechanism is small compared to the circulation transport mechanism (as derived below). Accordingly the governing differential equation for thermal energy balance at the tissue (Figure 5.2-1) is:

$$w_A c_B T_A - w_V c_B T_V = M c_M \frac{dT_M}{dt} \qquad (1)$$

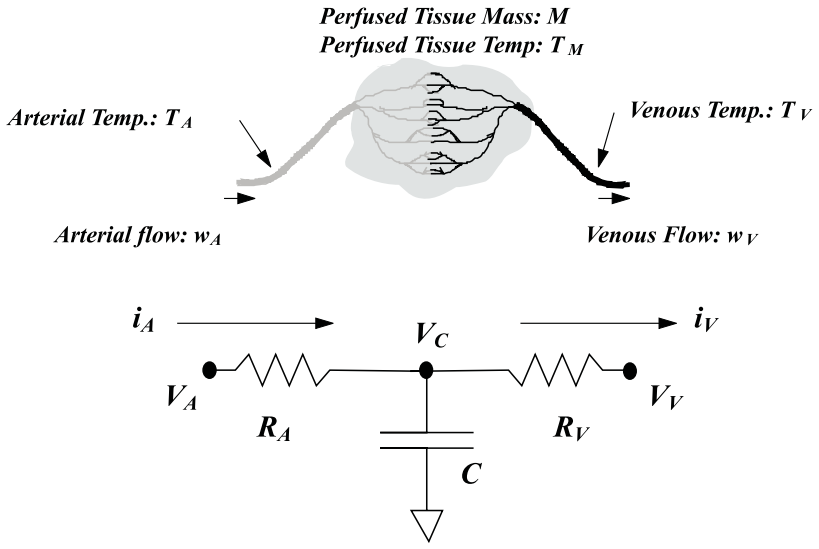

Figure 5.2-1. Derivation of governing differential equations for thermal transport and electrical analog.

Since the specific heats of blood (c_B) and tissue mass (c_M) are approximately the same; the arterial flow and venous flow are the same: and the tissue mass temperature is the same as venous temperature[8], then the equation can be simplified to:

$$T_A - T_M = T_A - T_V = \tau \frac{dT_M}{dt} \quad ; \textit{where} \quad \tau = \frac{Mc}{wc} \qquad (2)$$

The parameter τ can be referred to as the *thermal time constant.*

The electrical analog model employs the convention which substitutes electrical current flow for heat flow and voltage differences for temperature differences. Equation (2) can then be rewritten in its electrical analog form as:

$$V_A - V_C = V_A - V_V = \tau \frac{dV_C}{dt} \quad ; \textit{where} \quad \tau = RC \qquad (3)$$

Since the electrical capacitance ***C*** replaces the thermal capacitance ***Mc***, this result immediately leads to:

$$R_A = R_V = R \Rightarrow R = \frac{1}{wc} \tag{4}$$

Reviewing this result, due to its importance in thermal modeling, the governing equation is:

$$q = C\frac{dT}{dt} \Rightarrow i = C\ \frac{dV}{dt} \tag{5}$$

where ***q*** is the heat flow into the tissue, ***T*** the temperature of the tissue, and ***C*** is the thermal capacitance of the tissue (sometimes incorrectly described as the thermal inertia). The electrical analog symbols are conventionally ***i*** for current ***C*** for capacitance, and ***V*** for voltage.

The interconnecting vasculature transport resistance was derived with the following reasoning. The governing equation for heat transport via a fluid is:

$$q = wc\left(T_1 - T_2\right) \tag{6}$$

where ***w*** is mass flow rate, ***c*** is specific heat, T_1 and T_2 are upstream and downstream temperatures respectively, and ***q*** is interpreted as positive when heat is transported from a fluid at T_1 higher than fluid T_2 . The analogous electrical equation

$$i = \frac{1}{R}\left(V_1 - V_2\right) \tag{7}$$

leads directly to

$$R = \frac{1}{wc} \tag{8}$$

Examining (4) or (8) and testing its limits, the thermal transport resistance is zero at infinite fluid flow rate and infinite at zero fluid flow (heat diffusion via conduction is not included), which is a correct result.

However, there is the problem of flow direction to assess. The heat trans-

port equation does not specify a direction, but only that heat is transported down its temperature gradient, not its pressure gradient. Accordingly, if fluid were flowing from a colder T_1 to a warmer T_2 , the result would be a negative q. Similarly, if the fluid were to reverse and flow from a warmer T_2 to a colder T_1, the result is the same negative q.

The surprising counter-intuitive result is that the connecting vasculature can be mathematically modeled with simple resistors, whose values are inversely proportional to mass flow rate.

The circuit was designed element by element and "built" in an electrical simulation computer program.[9] The thermal elements were scaled electrically as follows:

TABLE 5.2-1. ELECTRICAL ANALOG CONVERSION

Thermal Parameter	*Quantity*	*Electrical Analog*
Heat Flow	1 BTU/sec (0.25 kcal/sec)	1 mV of voltage
Temperature	1°F (0.56°C)	1 mA of current
Resistance	1°F/BTU/sec (2.2°C/kcal/sec)	1 Ohm of resistance
Heat Capacity	1 BTU/°F (0.45 kcal/°C)	1 Farad of capacitance

The properties of water were used throughout since water is a reasonable model for thermal properties of living tissue, and none of the results were particularly sensitive to properties. Estimates of mass distribution, metabolism distribution, and skin heat transfer coefficient likewise showed no signs of sensitivity in affecting results, and therefore, modelling estimates of each were made as follows:

TABLE 5.2-2. TISSUE PARAMETER ESTIMATES

Tissue	*Mass*	*Resting Metabolism*	*Heat Transfer Coefficient*
Skin of Head 1 ft² (0.1 m²)	2 lb (1 kg)	—	2 Btu/hr-ft²-°F (10 Watts/m²-°C)
Head	5 lb (2.5 kg)	0.02 Btu/sec (20 Watts)	— —
Internal Tissue	75 lb (34 kg)	0.04 Btu/sec (40 Watts)	— —
Muscles	50 lb (23 kg)	0.04 Btu/sec (40 Watts)	—
Skin of Body 10 ft² (1 m²)	20 lb (9 kg)	—	2 Btu/hr-ft²-°F (10 Watts/m²-°C)

The electrical capacitance values for each are set numerically equal to the mass (English units). The estimates for mass flow rates are included in the resistance values shown in the circuit elements. For example, the carotid artery and jugular vein are estimated to carry about .034 lb/sec (1 L/min) blood flow, resulting in resistances of ***30 ohms***.

Tissue-to-tissue thermal diffusion by conduction was ignored, since the equivalent diffusion resistance is

$$R_D = \frac{x}{kA} \qquad (9)$$

where x is conduction distance, k thermal conductivity, and A cross sectional area. To move heat energy a distance of one foot (30 cm) across one square foot (900 cm²) results in a resistance value of about ***10K ohms***. Since the flow transport resistances are two to three orders of magnitude smaller, heat diffusion by conduction was ignored.

Metabolic heat sources were electrically modeled as current sources formed by a large voltage source (1 Volt) into a large resistor, with the heat energy injected into the capacitance node, simulating metabolizing tissue. Small metabolic rates of vasculature and skin were lumped in with the adjoining tissue mass. The topological layout of the electrical circuit analog follows the general topology of the tissue location and cardiovascular system, for ease of simulation and analysis (Figure 5.2-2).

The model was tested against data obtained over the several years in clinical studies, surgical observations and sports medicine studies. Conventional temperatures were taken with standard clinical instrumentation in use by medical personnel, and tympanic temperatures with infrared devices,[5] unless otherwise indicated.

Results and Discussion

The mathematical simulation is brought to "life" in Figure 5.2-2 by starting it from cold. Rectal (Re), pulmonary artery (PA), and tympanic (TM) all read 35 mV above zero ambient in steady state, which scales to 35°F (19°C) above ambient, and is close to reality for arterial temperature. Skin temperature is about 9°F (5°C) lower than arterial, which is also realistic. The 15 hour time constant results from the requirement to warm a mass of 70 kg with a resting metabolic rate of approximately 100 Watts.

Figure 5.2-3 shows the comparison between actual data and the model prediction for an infusion of 100 cc/min of iced saline into the vena cava of a volunteer.[10] The model predicts the same temperature depression as actually measured - about 2°C drop in 15 minutes.

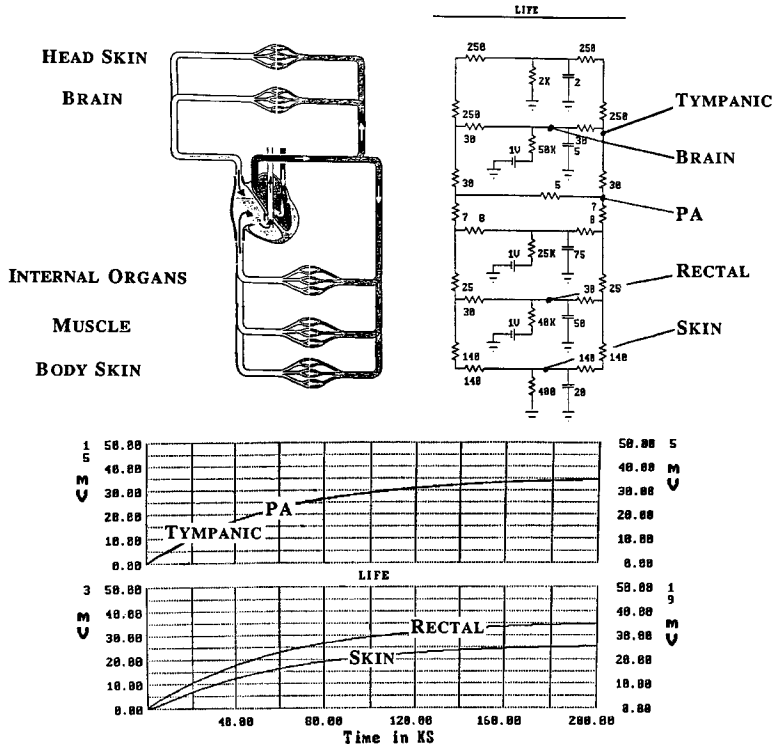

RESISTORS: $R = 1/wc$; W = PERFUSION RATE, C = SPECIFIC HEAT

CAPACITORS: $q = C\dfrac{dT}{dt}$; Q = HEAT FLOW, $\dfrac{dT}{dt}$ = TEMPERATURE RATE OF CHANGE

TEMPERATURE SCALING: 1MV = 1°F (0.6°C) ABOVE AMBIENT. FOR NORMAL 68°F (20°C) AMBIENT, 30 MV = 98°F (37°C).

CURRENT SCALING: 1MA = 1 BTU/SEC (.25 KCAL/SEC)

TIME SCALING: SIMULATION CHARTS IN KS (KILOSECONDS

Figure 5.2-2. Thermal transport simulation being "brought to life" from cold by turning on resting metabolism of 100 Watts at time = 0. PA and TM temperatures are essentially identical, Re is warmer than Sk. Warm-up time constant is ~ 15 hrs (54 kilosec).

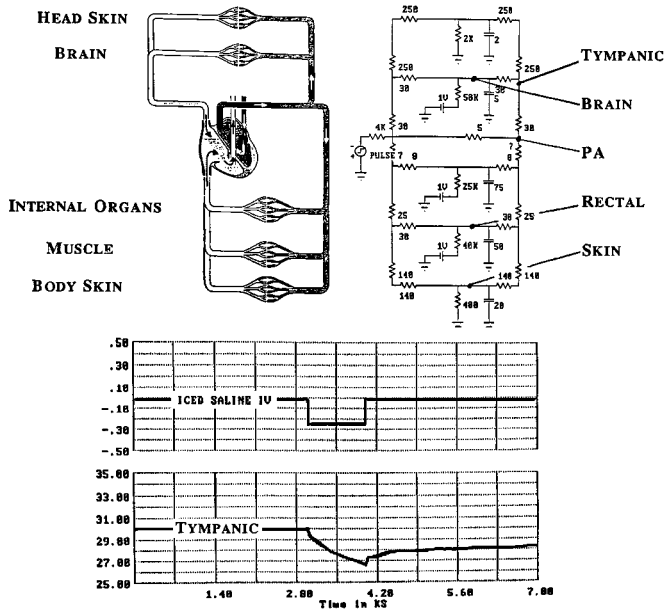

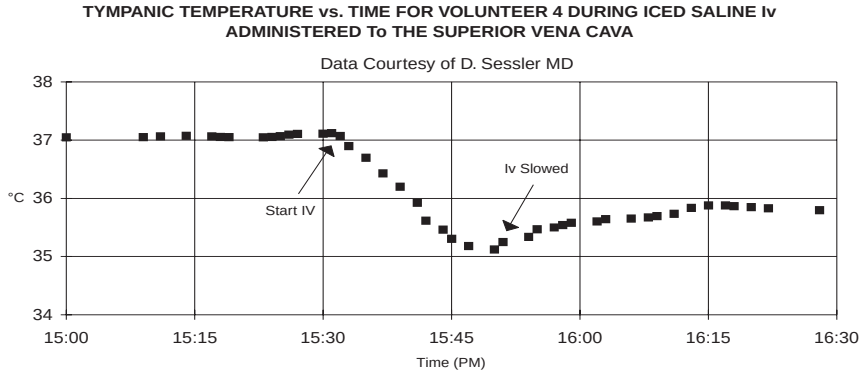

Figure 5.2-3. Comparison between model simulation and actual data for 100 cc/min. iced saline infusion. The simulation models the cold IV bolus as a pulse of negative current flow (top simulation curve), which results in the predicted tympanic temperature profile (lower simulation curve). The actual data is seen to closely agree with the simulation: approximately 2°C drop about 15 minutes (~1 Ksec) after IV start.

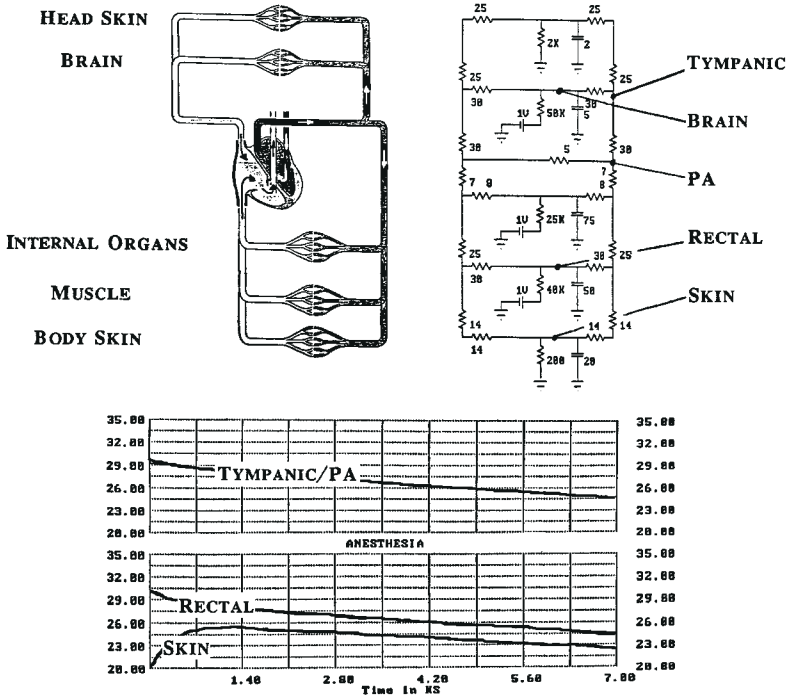

PULMONARY ARTERY AND TYMPANIC TEMPERATURES POST-ANASTHESIA AND PRE-BYPASS FOR CABG PATIENT

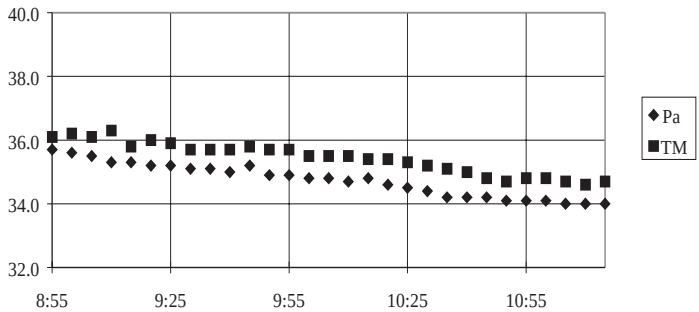

Figure 5.2-4. Comparison between model and data for characteristic cooling associated with thermal inversion caused by general anesthesia. The simulation model predicts about 2°C reduction in PA and TM temperature over a 2 hour (~ 7 Ksec) period, which agrees with the actual observation, thus supporting the inversion hypothesis.

Figure 5.2-4 shows the typical cooling of a surgical patient under general anesthesia, which commonly leads to surgical hypothermia. This cooling is believed to be caused by a thermal "inversion" created by vasodilation initiated by the anesthesia, resulting in warm arterial blood flowing to the periphery and cool peripheral blood flowing to the core[11]. The model simulates the metabolic and hemodynamic effects of the anesthesia by reducing heat generation by half to account for the lowered resting metabolism, and by increasing body skin blood flow by a factor of ten to simulate vasodilation. The model reproduces the characteristic cooling in both magnitude and dynamics and, therefore, supports the inversion hypothesis.

Another surgical example is Figure 5.2-5, showing a coronary artery bypass graft (CABG) patient undergoing cooling and heating via cardiopulmonary bypass[13]. The simulation models heat flow in the upper chart, which is the product of bypass flow and arterio-venous temperature difference. In the plateau section between heating and cooling, low temperature is maintained during the surgical procedure. The mathematical model performs well at predicting both the general features and quantitative temperature differences.

Figure 5.2-6 is data taken on a hyperthermic runner having just completed a 3 mile race in warm humid weather[14] . As the data shows, his tympanic temperature actually increased while he sat in the medical tent. His temperature continued to increase, placing him in danger of heat injury until he applied ice to his forehead and face. The immediate drop in tympanic temperature was accompanied by his regaining mental acuity and he left the tent. The model simulation is set to start the rectal (muscle) temperature at 40 mV instead of 30 mV, which is about 5°C higher than normal and consistent with many observations of high rectal temperatures on athletes after exercise[15] . The simulation result reproduces the data surprisingly well, which supports the hypothesis that the runner was under attack from his own heat stored in his lower muscles when cooling is inadequate.

The runner of Figure 5.2-7 had just completed the Boston Marathon. His rectal temperature, at 42°C was in a clinically dangerous zone, if interpreted conventionally. However, the tympanic temperature showed normal. As cooling was applied to his face and head, both temperatures began to fall, with Re and TM trending toward convergence. As in the simulation of Figure 5.2-6, the initial condition for Re was set 5°C higher than the other tissue capacitor nodes, resulting in a simulation that reproduces the actual data. The runner's 42°C was a result of local muscle temperature and of no clinical concern unless the heat were transported to the brain via the circulation. The cooling administered was sufficient to prevent this heating, and after rest and fluids, the 42°C athlete simply walked out of the medical tent.

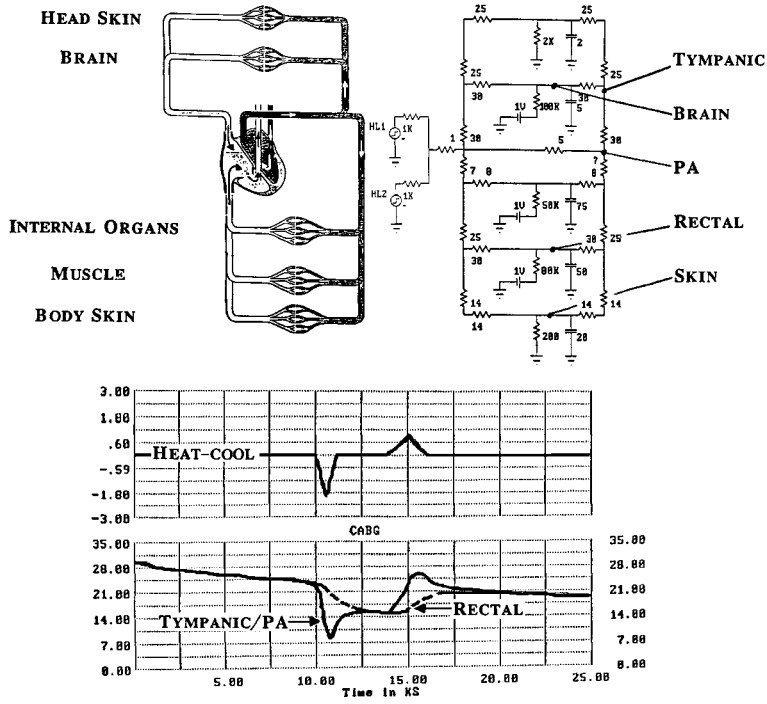

ESOPHAGEAL, PULMONARY ARTERY, BLADDER AND TYMPANIC TEMPERATURES DURING CABG PROCEDURE

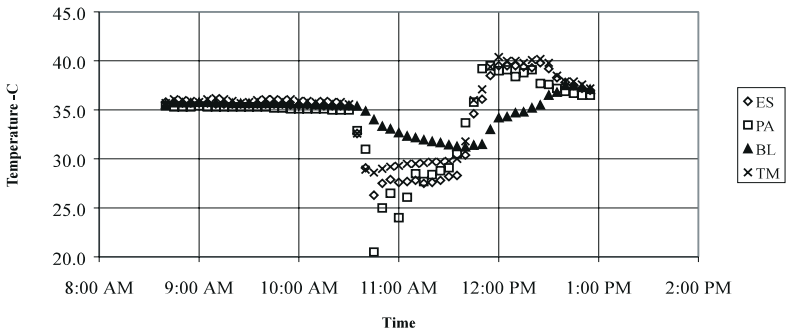

Figure 5.2-5. Comparison between model and actual data for a CABG patient undergoing cardiopulmonary bypass cooling and heating. The model cools then heats via appropriately scaled current flows (top simulation curve) and produces the temperatures (lower simulation curve). Actual data shows the same result as the simulation: PA and TM are fast to respond due to high perfusion per unit mass, while bladder and rectal are much slower due to much lower perfusion per unit tissue mass.

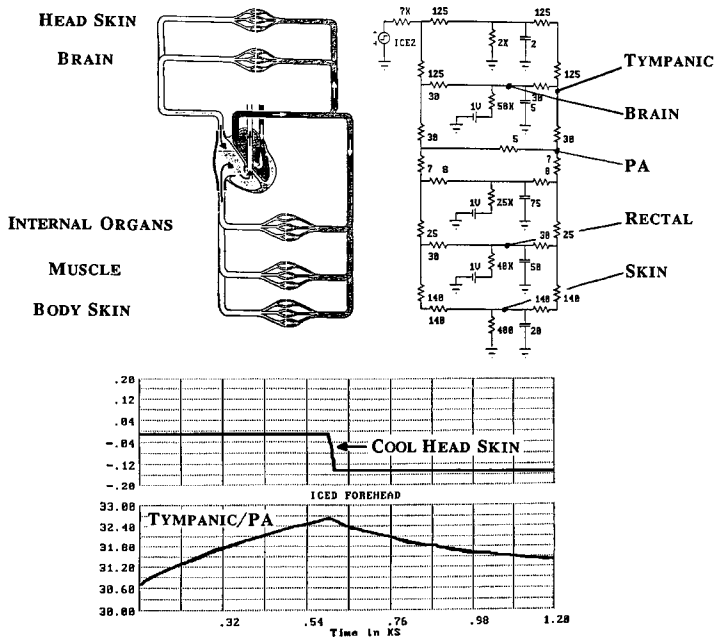

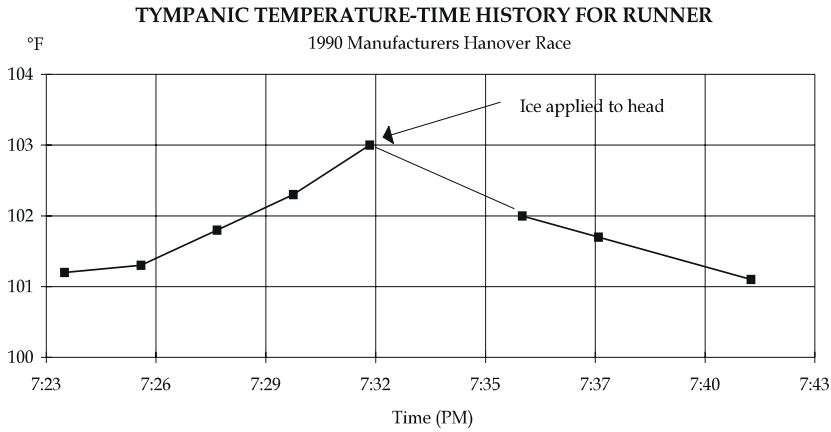

Figure 5.2-6. Comparison between model and data for a runner having completed a 3-mile race in warm humid weather. If cooling is inadequate and there is significant heat energy stored in the running muscles, the circulation will transport the heat to the head at a rate of about 2 °F (1°C) in 10 minutes. When adequate cooling is applied to the head only, the rate of temperature reduction is of the same magnitude, as confirmed by the data.

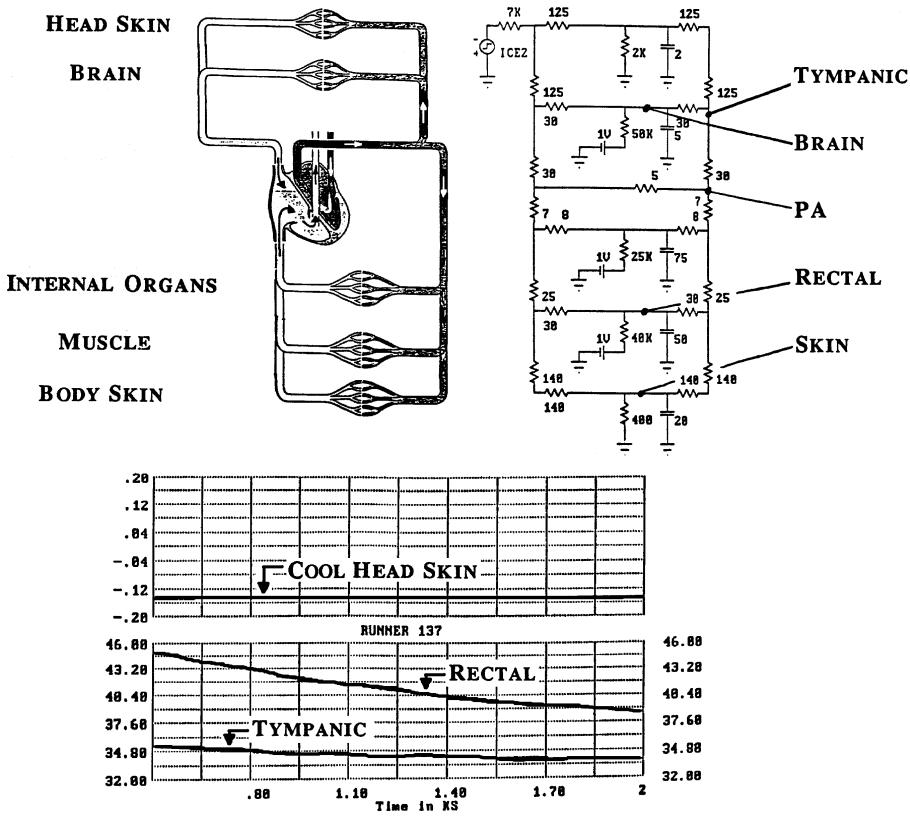

Figure 5.2-7. Model simulation predicts the observed temperature-time characteristics for a runner with significant heat storage in the running muscles and adequate cooling to the face and head. Rectal temperature reduces at a rate of about 2°C in 15 minutes, while TM cools at half that rate. *(Pompei, et al[16])*

The model performs extraordinarily well at predicting dynamic responses in the cases shown, namely the temperature distribution changes that occur in times that are long compared to circulation times, i.e. longer than a minute. For shorter times, for example, examining the thermodilution transient from the iced saline injection, the model cannot cope, since it has no time delay in its transport model. The simple resistor transport element properly moves the heat, but only for times long compared to the transit time of the blood.

The model and results suggest a striking analogy with thermoregulation systems familiar to all — those in our homes. In the conventional core/shell interpretation, heating is by a central hearth in the core, which radiates or conducts heat to the cooler periphery of the house. The model presented here suggests the far more efficient method of circulation. It seems that Mother Nature uses this method for the same reasons that our dwellings are designed this way - transport of heat via fluid circulation is most economic in space use, most efficient in power use, and most easily controlled compared to simple conduction/diffusion.

This article is adapted from a paper written by one of us (FP) at Harvard University, January 1993.

REFERENCES

[1] Benzinger, TH: Heat regulation: homeostasis of central temperature in man", *Physiological Reviews*, Vol 49, No. 4, October 1969.

[2] Boston Marathon Medical Team data taken 1989-95.

[3] Casey, J: Data prepared for publication, June 1992.

[4] Human Physiology, R.F. Schmidt, G. Thews (Eds), Second Edition, Springer Verlag 1989, p. 627.

[5] Ototemp 3000 Infrared Tympanic Thermometer, Exergen Corporation, Boston, MA.

[6] LighTouch Infrared Thermometer, Exergen Corporation, Boston, MA

[7] Microcap II Electronic Circuit Analysis Program, Spectrum Software, Sunnyvale, CA.

[8] Patton HD, Fuchs AF, Hille B, Scher AM, Steiner R. *Textbook of Physiology*, 21st Ed. vol 2, WB Saunders 1989.

[9] Microcap II Electronic Circuit Analysis Program, Spectrum Software, Sunnyvale, CA.

[10] Sessler, DI: Unpublished Data. University of California at San Francisco.

[11] Sessler DI, Ponte J: Hypothermia during epidural anesthesia results mostly from redistribution of heat within the body, not heat loss to the environment (abstract). *ANESTHESIOLOGY* 71:A882, 1989

[12] Sessler DI, Ponte J: Hypothermia during epidural anesthesia results mostly from redistribution of heat within the body, not heat loss to the environment (abstract). *ANESTHESIOLOGY* 71:A882, 1989

[13] Pompei, F., Tinney, R., Valeri, CR, Khuri, S: Unpublished Data.

[14] Pompei, F., Adner, M., Casey, J: Unpublished Data.

[15] *Exercise Physiology*, McArdle, Katch, Katch (Eds), Second Edition, Lea & Fibiger, 1986, p. 449.

[16] Pompei, F., Adner, M., Goldman, R., Casey, J: Unpublished Data.